Appl. Phys. A 33, 153–159 (1984)

Applied Physics A Solids and Surfaces

Photoacoustic Spectroscopy of Thin SiO_2 Films Grown on (100) Crystalline Si Substrates

A Thermal Interferometric Technique Complementary to Optical Interferometry

A. Mandelis, E. Siu, and S. Ho

Photoacoustics Laboratory, Department of Mechanical Engineering, University of Toronto, Toronto, Ontario, M5S 1A4 Canada
Toronto, Ontario, M5S 1A4, Canada

Received 10 October 1983/Accepted 1 December 1983

Abstract. Photoacoustic Spectroscopy (PAS) has been used to measure the thickness of thin SiO_2 films grown on (100) Si wafers. The data are in reasonable agreement with a simple theoretical model. It suggests that photoacoustic spectroscopy is complementary to optical interferometry, in that it is capable of giving quantitative estimates of thin transparent films on opaque substrates of low reflectivity via the transmitted fraction of the optical energy incident on the sample. Both theoretical and experimental results indicate that PAS can be very useful in the measurement of thin films on substrates of low reflectivity.

PACS: 68, 78

Photoacoustic Spectroscopy (PAS) has been used recently to study layered solid samples [1–4] and thin film coatings [5, 6]. All these studies were essentially exploratory in nature aiming to demonstrate the sensitivity of the photoacoustic probe to the presence of solid layers having different optical and/or thermal properties from their substrates. Conventional gas-microphone PAS systems were used and the capability of PAS to detect absorbing or transparent layers on absorbing or transparent substrates was established both experimentally [1–8] and theoretically [3, 4, 9, 10].

The important question concerning the ability of PAS to provide *quantitative* information about the thickness of surface layers has not been addressed in the literature to the authors' best knowledge. Nevertheless, PAS has been shown to be a sensitive probe of submicrometer film thicknesses. Kanstad and Nordal [11] used an open membrane PAS spectrophone design to demonstrate that photoacoustic spectroscopy is sensitive to the presence of an absorbing anodized Al_2O_3 barrier oxide film of ca. 440 Å thickness. These authors detected a PAS signal from this absorbing film, which they attributed to the Al–O stretching vibration upon excitation with ir light polarized with its electric vector in the plane of incidence.

This paper is concerned with the application of PAS to the acquisition of quantitative thickness data of transparent thin films on absorbing crystalline substrates. Traditionally this information has been obtained using conventional reflection spectroscopy [12], which requires highly reflecting, molecularly clean surfaces. Workers in PAS can take advantage of the simplicity of spectra acquisition procedures to reduce significantly the labor required for accurate thin-film thickness measurements. A case in point is the measurement of SiO_2 thicknesses grown on single crystalline Si wafers for purposes of microelectronic device applications. A photoacoustic interferometric theory will be developed, which takes into account the optical interferometric character of the PAS response from a (transparent thin layer) + (absorbing substrate) system. The general theory indicates that the photoacoustic signal magnitude carries information about the thickness of the thin layer. This photoacoustic interferometric technique is especially suited to probing thin films

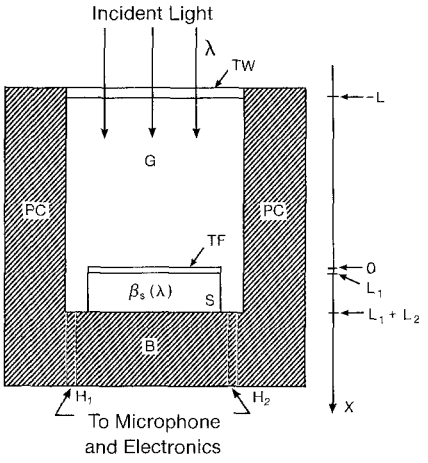

Fig. 1. Geometry for a double-layer, thin film-substrate, PAS system PC: photoacoustic cell; G: gas; TF: thin film; S: substrate; B: backing; H_1, H_2: drilled holes for sample chamber communication with microphone electronics; $\beta_s(\lambda)$: optical absorption coefficient of the substrate at light wavelength λ; TW: transparent window

on non-reflecting substrates, as it is only sensitive to radiation transmitted by the thin film. This kind of information is difficult or impossible to obtain via conventional optical interferometric methods (e.g., ellipsometry). The theory will be further compared with experimental results from (100) Si wafers with thermally grown films of SiO_2.

1. Theory

An idealized one-dimensional configuration of a photoacoustic system consisting of a thin transparent film on an absorbing substrate is shown in Fig. 1. The optical absorption coefficient $\beta_s(\lambda)$ of the substrate is a function of the wavelength of the incident radiation. The photoacoustic cell is hermetically sealed by a nonabsorbing thick window. We assume that the length L of the gas column above the sample is large compared to the thermal diffusion length μ_g in the gas. The sample is supported by a thick non-absorbing backing. Heat transfer between the solid and the gas following absorption and non-radiative conversion of the intensity-modulated light beam results in pressure fluctuations in the sample chamber which constitute the PAS signal. The light incident upon the solid is assumed to be modulated sinusoidally at an angular frequency ω_0. The transparent thin overlayer has a real index of refraction n_1, and the absorbing substrate has a complex refractive index $\hat{n}_2 = n_2 + ik_2$, where k_2 is the extinction coefficient of the substrate material. The notation $\hat{q}$ indicates complex quantities. The refractive index of the non-absorbing gas n_g, is that of air for most applications ($n_g = 1$).

1.1. The Optical and Thermal Problems

The photoacoustic signal is generated within the absorbing substrate S (Fig. 1) upon light transmission through the thin surface layer at the interface L_1. After p reflections at the film-gas and film-substrate boundaries at $x=0$ and $x=L$, respectively, the amplitude $E_p^{(T)}$ of the electric field vector of the transmitted light wave is given by the expression

$$\hat{E}_p^{(T)} = T_{01}\hat{T}_{12}(R_{10}\hat{R}_{12})^{p-1}\hat{E}_0 \exp[\mathrm{i}(p-\tfrac{1}{2})d_1], \tag{1}$$

where $\hat{E}_0$ is the amplitude of the electric field vector of the incident light wave, T_{01} and $\hat{T}_{12}$ are the transmission coefficients at the gasfilm (01) and film-substrate (12) interfaces; R_{10} and $\hat{R}_{12}$ are the reflection coefficients within the thin film at the gas (10) and substrate (12) interfaces. The constant d_1 is the phase difference between the p^{th} and the $(p-1)^{\text{th}}$ wave functions and corresponds to a double traversal of the thin film. For normal incidence this phase difference at wavelength λ is [13]

$$d_1 = \left(\frac{4\pi}{\lambda}\right) n_1 L_1 . \tag{2}$$

If the lateral dimension of the irradiated sample is large compared to the film thickness, the amplitude of the electric field vector of all the light transmitted to the substrate is given by

$$\hat{E}^{(T)} = \sum_{p=1}^{\infty} E_p^{(T)} = \hat{E}_0 \left(\frac{T_{01}\hat{T}_{12}\exp(\mathrm{i}d_1/2)}{1 - R_{10}\hat{R}_{12}\exp(\mathrm{i}d_1)} \right). \tag{3}$$

Light transmitted into the absorbing substrate may also be reflected at the substrate-film (21) and substrate-backing (2b) interfaces, especially in cases of highly reflective solids, such as Si crystals. After q reflections at the boundaries $x=L_1$ and $x=L_1+L_2$ the amplitude $E_q^{(R)}(x)$ of the electric field vector of the reflected light at a depth x inside the solid is

$$\hat{E}_q^{(R)}(x) = \hat{E}_q^{(R)}(x; L_1) + \hat{E}_q^{(R)}(x; L_1 + L_2), \tag{4}$$

where

$$\hat{E}_q^{(R)}(x; L_1) = \hat{E}^{(T)} \exp[\mathrm{i}\hat{D}_2(x)]\,[R_{2b}\hat{R}_{21}\exp(\mathrm{i}\hat{d}_2)]^{q-1} \tag{5}$$

and

$$\hat{E}_q^{(R)}(x; L_1 + L_2) = \hat{E}^{(T)}\hat{R}_{2b}\exp\{\mathrm{i}[\hat{d}_2 - \hat{D}_2(x)]\} \cdot [\hat{R}_{2b}\hat{R}_{21}\exp(\mathrm{i}\hat{d}_2)]^{q-1} \tag{6}$$

so that

$$\hat{E}_q^{(R)}(x) = \hat{E}^{(T)}(\exp[\mathrm{i}\hat{D}_2(x)] + \hat{R}_{2b}\exp\{\mathrm{i}[\hat{d}_2 - \hat{D}_2(x)]\}) \cdot [\hat{R}_{2b}\hat{R}_{21}\exp(\mathrm{i}\hat{d}_2)]^{q-1} . \tag{7}$$

In (6) and (7) $\hat{d}_2$ is the phase difference between the q^{th} and the $(q-1)^{\text{th}}$ wave functions in the substrate. For

normal incidence at wavelength λ

$$\hat{d}_2 = \left(\frac{4\pi}{\lambda}\right)\hat{n}_2 L_2 \tag{8}$$

and

$$\hat{D}_2(x) = \left(\frac{2\pi}{\lambda}\right)\hat{n}_2 x. \tag{9}$$

The following relationships are valid for the various reflection and transmission coefficients at the (i,j) interface [14]

$$\hat{R}_{ij} = -\hat{R}_{ji}, \tag{10}$$

$$\hat{T}_{ij} = (1-\hat{R}_{ji}^2)/\hat{T}_{ji}. \tag{11}$$

The amplitude of the electric field vector $\hat{E}(x)$ at depth x inside the substrate is given upon summing over all partial wave contributions at x

$$\begin{aligned}\hat{E}(x) &= \sum_{q=1}^{\infty} \hat{E}_q^{(R)}(x) \\ &= \hat{E}_0\left(\frac{\exp[\mathrm{i}\hat{D}_2(x)] + \hat{R}_{2b}\exp\{\mathrm{i}[\hat{d}_2 - D_2(x)]\}}{1-\hat{R}_{2b}\hat{R}_{21}\exp(\mathrm{i}d_2)}\right) \\ &\quad \cdot\left[\frac{T_{01}\hat{T}_{12}\exp(\mathrm{i}d_1/2)}{1-R_{10}\hat{R}_{12}\exp(\mathrm{i}d_1)}\right].\end{aligned} \tag{12}$$

Equation (12) can be used to obtain an expression for the light intensity at depth x [12]:

$$\begin{aligned}I(x) &= \frac{c}{4\pi}\frac{|\hat{n}_2|}{n_1}\hat{E}(x)\hat{E}^*(x) \\ &= \frac{c}{4\pi}\frac{|\hat{n}_2|}{n_1}(\hat{E}_0\hat{E}_0^*) \\ &\quad \cdot\left(\frac{|\exp[\mathrm{i}\hat{D}_2(x)]|^2|\hat{Z}_1|^2}{|\hat{Z}_2|^2}\right)\frac{T_{01}^2|\hat{T}_{12}|^2}{|\hat{Z}_3|^2},\end{aligned} \tag{13, 14}$$

where

$$\hat{Z}_1 \equiv 1 + \hat{R}_{2b}\exp\{\mathrm{i}[\hat{d}_2 - 2\hat{D}_2(x)]\}, \tag{15}$$

$$\hat{Z}_2 \equiv 1 - \hat{R}_{2b}\hat{R}_{21}\exp(\mathrm{i}\hat{d}_2), \tag{16}$$

and

$$\hat{Z}_3 \equiv 1 - R_{10}\hat{R}_{12}\exp(\mathrm{i}d_1). \tag{17}$$

The complex quantities $\hat{R}_{jk}$ and $\hat{T}_{jk}$ can be written in polar coordinates:

$$\hat{R}_{jk} = |\hat{R}_{jk}|\exp(\mathrm{i}\phi_{jk}); \quad \hat{T}_{jk} = |\hat{T}_{jk}|\exp(\mathrm{i}\theta_{jk}), \tag{18}$$

where [12]

$$\begin{aligned}R_{10} &= (n_1 - n_g)/(n_1 + n_g) \\ &= (n_1 - 1)/(n_1 + 1) \quad \text{for} \quad g = \text{air}.\end{aligned} \tag{19}$$

In general,

$$\hat{R}_{jk} = (\hat{n}_j - \hat{n}_k)/(\hat{n}_j + \hat{n}_k). \tag{20}$$

For the transmission coefficients we can write

$$T_{01} = 2n_g/(n_1 + n_g) = 2/(n_1 + 1) \quad \text{for} \quad g = \text{air} \tag{21}$$

and, in general:

$$\hat{T}_{jk} = 2\hat{n}_j/(\hat{n}_j + \hat{n}_k). \tag{22}$$

Using the relationship

$$\beta_s(\lambda) = 4\pi k_2(\lambda)/\lambda \tag{23}$$

in (9) between the optical absorption coefficient and the extinction coefficient of the substrate material, (14)–(17) can be written in the form

$$I(x) = I_0\frac{|\hat{n}_2|}{n_1}\exp[-\beta_s(\lambda)x]\left(\frac{|\hat{Z}_1|}{|\hat{Z}_2|}\right)^2\frac{T_{01}^2|\hat{T}_{12}|^2}{|\hat{Z}_3|^2} \tag{24}$$

with

$$I_0 \equiv \frac{c}{4\pi}|\hat{E}_0|^2 \tag{25}$$

and

$$\begin{aligned}|\hat{Z}_1|^2 &= 1 + 2|\hat{R}_{2b}|\exp[-\beta_s(L_2 - x)]\cos Q_1(x) \\ &\quad + |\hat{R}_{2b}|^2\exp[-2\beta_s(L_2 - x)],\end{aligned} \tag{26a}$$

$$\begin{aligned}|\hat{Z}_2|^2 &= 1 + 2|\hat{R}_{2b}\hat{R}_{12}|\exp(-\beta_s L_2)\cos Q_2 \\ &\quad + |\hat{R}_{2b}\hat{R}_{12}|^2\exp(-2\beta_s L_2),\end{aligned} \tag{26b}$$

$$|\hat{Z}_3|^2 = 1 - 2R_{10}|\hat{R}_{12}|\cos(d_1 + \phi_{12}) + R_{10}^2|\hat{R}_{12}|^2, \tag{26c}$$

where

$$Q_1(x) = \phi_{2b} + (4\pi n_2/\lambda)(L_2 - x)$$

and

$$Q_2 = \phi_{2b} + \phi_{12} + 4\pi n_2 L_2/\lambda.$$

1.2. A Special Practical Case of the Thermal Problem: The SiO_2:Si System

For the case of a crystalline Si substrate, the sample is optically opaque in the wavelength range of experimental interest (200–1000 nm). At these wavelengths [15, 16]

$$\beta_s(\lambda)L_2 \gg 1$$

for thicknesses L_2 typical of Si wafers (ca. 5×10^{-2} cm). This relation shows that for Si substrates, (26a, b) become

$$|\hat{Z}_1| \cong |\hat{Z}_2| \cong 1 \tag{27}$$

so that the light intensity at depth x within the bulk of the SiO_2:Si sample can be written:

$$\begin{aligned}I(x,t) &= I_0\frac{|\hat{n}_2|}{n_1}\left(\frac{T_{01}^2|\hat{T}_{12}|^2}{|\hat{Z}_3|^2}\right) \\ &\quad \cdot\exp[-\beta_s(\lambda)x]\,\mathrm{Re}\{1 + \exp(\mathrm{i}\omega_0 t)\}\; x \geqq L_1.\end{aligned} \tag{28}$$

The harmonic modulation of the light beam at angular frequency ω_0 results in rapidly damped, traveling thermal waves in the sample [17, 18].
Summing up the partial thermal waves transmitted from the substrate through the thin surface film to the surrounding gas, the complex temperature magnitude $\hat{\theta}^{(T)}(O)$ at the film surface is given by [Ref. 9, Eq. (16)]. This is also the two-layer extension of the thermal wave theory presented in [18]:

$$\begin{aligned}\hat{\theta}^{(T)}(O)=&\left(\frac{I_{\mathrm{eff}}(\lambda)\beta_s b_{12}}{K_2(\beta_s^2-\hat{\sigma}_2^2)}\right)[(\hat{r}_2-1)(b_{2b}+1)\\&\cdot\exp(\hat{\sigma}_2L_2)-(\hat{r}_2+1)(b_{2b}-1)\\&\cdot\exp(-\hat{\sigma}_2L_2)+2(b_{2b}-\hat{r}_2)\\&\cdot\exp(-\beta_sL_2)]/[(1+b_{1b})(1+b_{2b})\\&\cdot\exp(\hat{\sigma}_1L_1+\hat{\sigma}_2L_2)+(b_{12}-1)(b_{2b}+1)\\&\cdot\exp(-\hat{\sigma}_1L_1+\hat{\sigma}_2L_2)+(b_{2b}-1)(b_{12}+1)\\&\cdot\exp(-\hat{\sigma}_1L_1-\hat{\sigma}_2L_2)+(b_{12}-1)(b_{2b}-1)\\&\cdot\exp(\hat{\sigma}_1L_1-\hat{\sigma}_2L_2)],\end{aligned}\tag{29}$$

where

$$I_{\mathrm{eff}}(\lambda)\equiv I_0\frac{|\hat{n}_2|}{n_1}\left(\frac{|\hat{Z}_1|^2}{|\hat{Z}_2|^2}\right)\frac{T_{01}^2|\hat{T}_{12}|^2}{|\hat{Z}_3|^2}\tag{30}$$

and

$$b_{ij}\equiv K_j\hat{\sigma}_j/K_i\hat{\sigma}_i=\left(\frac{\varrho_jC_jK_j}{\varrho_iC_iK_i}\right)^{1/2}.\tag{31}$$

ϱ_i, C_i are, respectively, the density [g/cm^3] and the specific heat [Joules/g−K] of material (i). K_i is the thermal conductivity [W/cm−K] of (i).
Further,

$$\hat{r}_2\equiv(1-i)(\beta_s/2a_2)\tag{32}$$

and

$$\hat{\sigma}_j\equiv(1+i)\,a_j,\quad\text{where}\quad a_j\equiv(\omega_0/2\alpha_j)^{1/2}\tag{33}$$

α_j is the thermal diffusivity [cm^2/s] of material (j).
The pressure rise ΔP in the sample chamber due to the heat transmitted to the gas from the thin film surface is proportional to $\hat{\theta}^{(T)}(O)$ [19]. The complex photoacoustic signal is

$$\Delta\hat{P}(t)=\left(\frac{\gamma P_0\exp[\mathrm{i}(\omega_0t-\frac{1}{4}\pi)]}{\sqrt{2}La_gT_0}\right)\hat{\theta}^{(T)}(O)\tag{34}$$

and the amplitude of $\Delta\hat{P}(t)$ is

$$S\equiv|\Delta\hat{P}(t)|=Y|\hat{\theta}^{(T)}(O)|;\qquad Y\equiv\gamma P_0/\sqrt{2}La_gT_0,\tag{35}$$

where γ is the ratio of the specific heats, and L the (one-dimensional) volume of the sample chamber.

Crystalline silicon is a highly reflecting, optically opaque material, so that $\exp[-\beta_s(\lambda)L_2]\cong 0$. Due to its high thermal diffusivity ($\alpha_{si}=1.06\,\mathrm{cm}^2/\mathrm{s}$ [20]) it is also thermally thin at modulation frequencies below 50 Hz. Thin grown SiO_2 films of thickness $L_1\leqq 1\,\mu$m are optically transparent and thermally thin:

$$\beta_{\mathrm{SiO_2}}(\lambda)\cong 0,\exp(\pm\hat{\sigma}_{\mathrm{SiO_2}}L_1)=1.\tag{36}$$

In these limits, (35) can be simplified to

$$\begin{aligned}S_{\mathrm{SiO_2:Si}}=&Y\left(\frac{I_{\mathrm{eff}}(\lambda)}{2\sqrt{2}K_2\alpha_2}\right)\\&\cdot\left|\frac{(b_{2b}+1)\exp(\hat{\sigma}_2L_2)-(b_{2b}-1)\exp(-\hat{\sigma}_2L_2)}{(b_{2b}+1)\exp(\hat{\sigma}_2L_2)+(b_{2b}-1)\exp(-\hat{\sigma}_2L_2)}\right|.\end{aligned}\tag{37}$$

Equation (37) indicates that the magnitude of the PAS signal from the SiO_2:Si system is expected to be saturated, i.e. independent of $\beta_s(\lambda)$, yet a λ-dependence is apparent in the term $I_{\mathrm{eff}}(\lambda)$. This term can be isolated from the remaining terms in (37) upon normalization of $S_{\mathrm{SiO_2:Si}}$ by S_{Si}. The plain Si sample must be of thickness L_2 and in contact with the same backing support (B). In that case the sample-dependent terms $\hat{\sigma}_2$, L_2, b_{2b}, K_2 and the geometry-dependent Y term cancel out of the normalized signal magnitude to give the simple expression:

$$r(\lambda)\equiv\frac{S_{\mathrm{SiO_2:Si}}}{S_{\mathrm{Si}}}=\frac{I_{\mathrm{eff}}^{(\mathrm{SiO_2:Si})}(\lambda)}{I_{\mathrm{eff}}^{(\mathrm{Si})}(\lambda)}.\tag{38}$$

From (27, 28, and 30), and considerations similar to those of Part (A), we find

$$I_{\mathrm{eff}}^{(\mathrm{SiO_2:Si})}(\lambda)\cong(T_{01}^2|\hat{T}_{12}|^2/|\hat{Z}_3|^2)\left(\frac{|\hat{n}_2|}{n_1}\right)I_0\tag{39}$$

and

$$I_{\mathrm{eff}}^{(\mathrm{Si})}(\lambda)=|\hat{T}_{02}|^2\left(\frac{|\hat{n}_2|}{n_g}\right)I_0.\tag{40}$$

Equations (38–40) give the normalized PAS signal magnitude

$$r(\lambda)=\frac{(n_g/n_1)}{|\hat{Z}_3|^2}\left(\frac{T_{01}|\hat{T}_{12}|}{|\hat{T}_{02}|}\right)^2.\tag{41}$$

Equation (26c) shows that maxima of $|\hat{Z}_3|^2$ occur at values of $(d_1+\phi_{12})$ such that

$$d_1+\phi_{12}=(2m+1)\pi;\qquad m=0,1,2,\ldots.\tag{42}$$

For these values we obtain

$$r(\lambda)\Big|_{\min}=\left(\frac{n_g}{n_1}\right)\left(\frac{T_{01}|\hat{T}_{12}|}{(R_{10}|\hat{R}_{12}|+1)|\hat{T}_{02}|}\right)^2.\tag{43}$$

Minima of $|\hat{Z}_3|^2$ occur at values of $(d_1+\phi_{12})$ such that

$$d_1+\phi_{12}=2m\pi;\qquad m=0,1,2,\ldots.\tag{44}$$

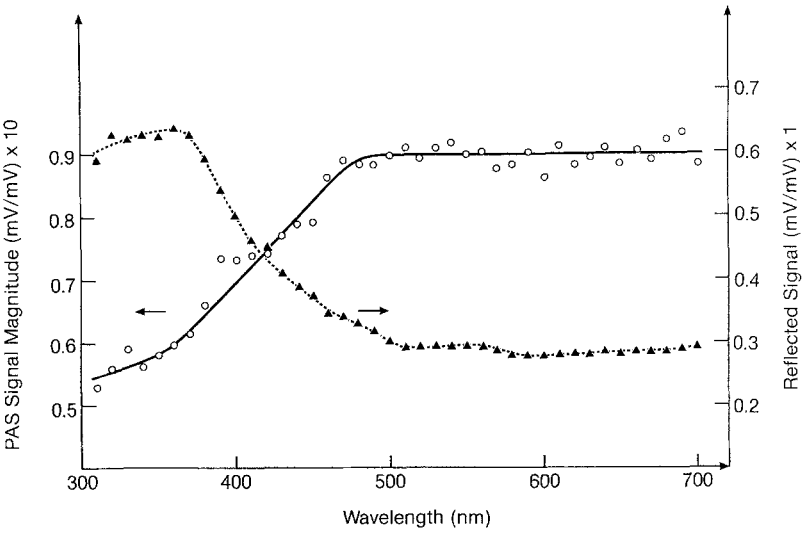

Fig. 2. Photoacoustic (○) and reflectance (△) spectra from a Si (100) surface. The PAS spectrum was normalized by the Xe lamp spectrum using Xerox toner. (Resolution: 8 nm; modulation frequency: 50 Hz; lock-in time constant: 3 s

For these values we obtain

$$r(\lambda)\Big|_{\max} = \left(\frac{n_g}{n_1}\right)\left(\frac{T_{01}|\hat{T}_{12}|}{(R_{10}|\hat{R}_{12}|-1)|\hat{T}_{02}|}\right)^2. \tag{45}$$

Equations (43) and (45) confirm that photoacoustic minima (maxima) occur for values of $(d_1+\phi_{12})$ corresponding to optical reflection maxima (minima) obtained from thin transparent films [13]. The thickness L_1 of the thin film can be obtained from two consecutive PAS minima (or maxima), using (43), or (45). If two consecutive extrema occur at wavelengths λ_1 and λ_2, such that $\lambda_1 > \lambda_2$, the thin film thickness can be determined photoacoustically from the simple relation:

$$L_1 = \frac{2\pi+\phi_{12}(\lambda_1)-\phi_{12}(\lambda_2)}{4\pi\left(\frac{n_1(\lambda_2)}{\lambda_2}-\frac{n_1(\lambda_1)}{\lambda_1}\right)}; \quad \lambda_1 > \lambda_2. \tag{46}$$

2. Experimental

The materials used in this work were (100)-oriented, polished Si wafers from S.E.H. America (7.5 cm, *p*-type, average nominal resistivity 15.5 Ω-cm), and from Semi-Metals Corp. (5 cm, *n*-type, 1–2 Ω-cm nominal resistivity). The wafers were cleaned prior to oxidation using the standard RCA clean, and subsequently oxidized at 1100 °C to form gate (ca. 1000 Å), and field (ca. 9000 Å) oxides. A few substrates were also thermally oxidized to ca. 5000 Å thickness. After the oxidation, the wafers were cut with a diamond-tipped scribe so as to fit into the sample compartment of an EG&G Model 6003 photoacoustic cell. PAS spectra were taken using a 1000 W Xe lamp from Oriel, and 2 mm (8 nm resolution) slitwidth. Both the photoacoustic magnitudes and phases were recorded, using an EG&G 5204 lock- in analyzer. Optical reflection spectra were also recorded from unoxidized and oxidized wafers, using the PAS system light source and monochromator, with a Moll Thermopile detector (Kipp & Zonen).

3. Results and Discussion

Figure 2 shows reflection and photoacoustic spectra recorded from an S.E.H. unoxidized Si wafer. The wafer had been etched to hydrophobia for ca. 15 s to eliminate any spectral effects due to native oxides. The PAS data appear noisier than the reflection data due to the higher signal strength of the reflection spectra. Figure 2 indicates quite clearly the expected anticorrelation between PAS and reflection curves. The normalized photoacoustic magnitude exhibits a strong wavelength dependence in the spectral region from 300 to 500 nm. In this region the optical absorption coefficient for Si ranges between 10^4 and $2\times10^6\,\mathrm{cm}^{-1}$ [15], and the PAS signal is normally expected to be saturated [19]. The signal dependence on λ must be attributed to $I_{\mathrm{eff}}(\lambda)$ of (30).

Figure 3 shows reflection and photoacoustic spectra from a field oxide grown on an S.E.H. wafer. The well-known [12] interference patterns of the reflection data anticorrelate very well with PAS thermal interference patterns, as predicted by (43 and 45). Figure 3 demonstrates that photoacoustic spectroscopy can be used as an interferometric technique to give information about thin films on surfaces. The comparison between optical and photoacoustic fringes (maxima and minima), and simple energy conservation arguments based on the theoretical discussion in this paper, indicate that PAS can be a valuable tool for the study of thin films grown

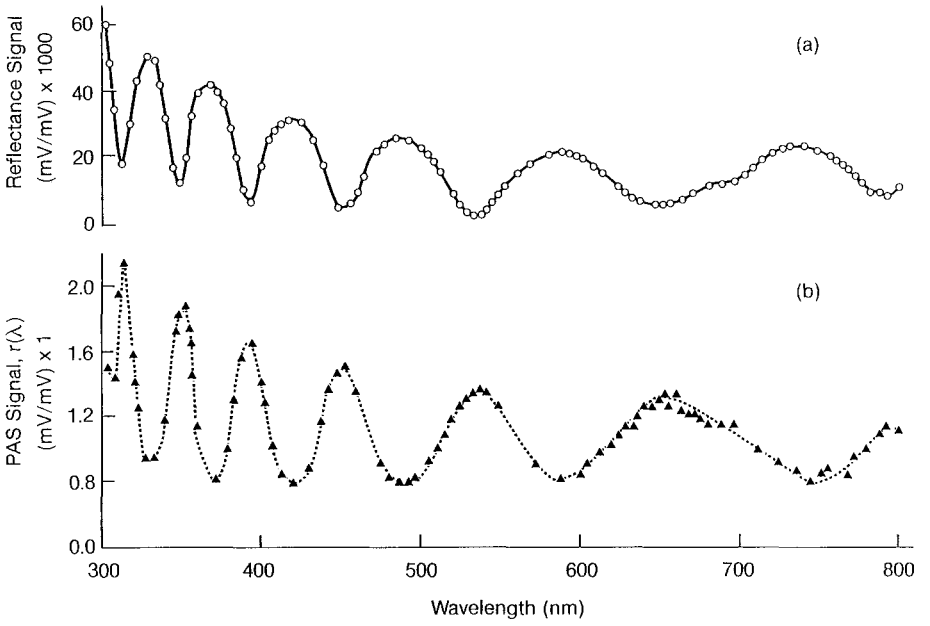

Fig. 3. (a) Reflectance spectrum from a grown oxide (ca. 9000 Å thickness) on a Si wafer, normalized by the reflectance spectrum of Si, Fig. 2. (b) PAS spectrum from the same oxide, normalized by the Si spectrum (unnormalized). (Resolution: 8 nm; modulation frequency: 50 Hz; lock-in time constant: 3 s

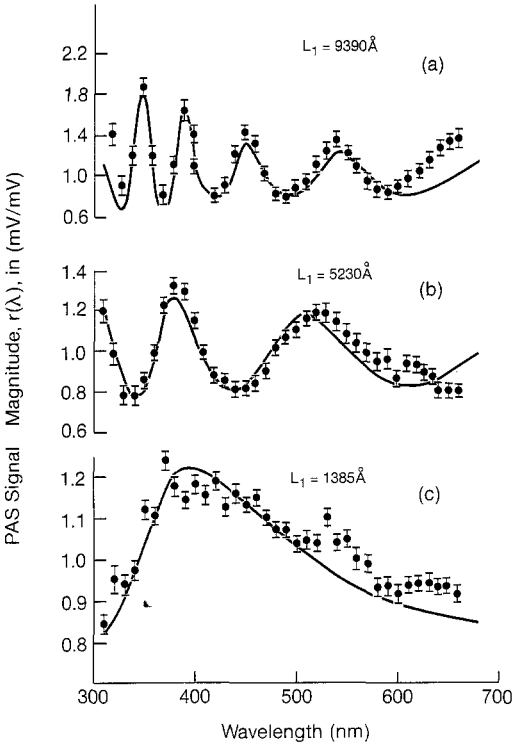

Fig. 4a–c. Photoacoustic interference spectra from oxidized wafers, normalized by the Si spectrum obtained after oxide etch; (○): Experimental points; (−): Least squares fits to (41). (a) 9000 Å grown SiO_2; (b) 5000 Å; (c) 1000 Å. Optimized theoretical thicknesses are indicated on each plot. (Resolution: 8 nm, modulation frequency: 50 Hz; lock-in time constant: 3 s

or deposited on opaque substrates which have poor reflection properties. In that case the transmitted fraction of the incident light is expected to increase at the expense of the reflected fraction, thus increasing the overall photoacoustic interference signal.

Figure 4 shows experimental photoacoustic results from oxidized S.E.H. ($L_1 = 9390$ Å) and Semi-Metals ($L_1 = 5230$ Å, 1385 Å) wafers. The continuous lines are least squares fits to the data, using (41). In the calculation of the theoretical curves, n_1 was set equal to the refractive index of fused silica, known to be real for energies below 8.9 eV [21] and a complicated function of wavelength [22]:

$$n_1^2(\lambda) = 1 + \frac{0.6961663\lambda^2}{\lambda^2 - (0.0684043)^2} + \frac{0.4079426\lambda^2}{\lambda^2 - (0.1162414)^2} + \frac{0.8974794\lambda^2}{\lambda^2 - (9.896161)^2}, \tag{47}$$

where λ is in μm.

The optical constants n_2 and k_2 for silicon were calculated from [15, 16] and used to find numerical values for $|\hat{Z}_3|^2$, Eq. (26c). The computer fits to the data in Fig. 4, when optimized with the oxide thickness L_1 as a parameter, show good agreement in the 300–600 nm region. The accuracy of the numerical results from (41) is essentially limited by our ability to read the values of n_2 and k_2 off the absorption curves for silicon presented in [15, 16]. The seemingly simpler, alternative method of calculating L_1 from the minima/maxima of the interference spectrum of Fig. 4 using (46), proved to be much less accurate in practice, due to the large uncertainties involved in the determination of the exact spectral position of two consecutive extrema. The deviation of the theoretical curves from the data points for $\lambda \geqq 550$ nm, apparent in Fig. 4 has been previously observed in the reflectance spectrum of thin oxide films on Si ($L_1 < 3000$ Å) by Powell [23]. Powell attributed this deviation to error in the optical constants of the thin (90 Å) gold electrode attached to the

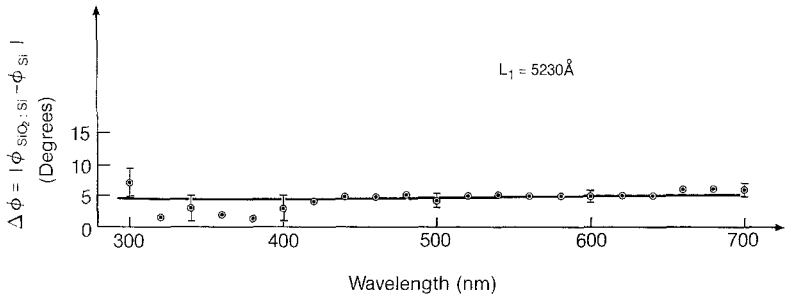

Fig. 5. Photoacoustic phase difference between oxidized and subsequently etched Si wafer of Fig. 4b. (Resolution: 8 nm; modulation frequency: 50 Hz; lock-in time constant: 3 s

oxide of his SiO_2:Si sample for photoinjection measurements. The present data indicate that the origin of the deviation lies elsewhere. Powell also calculated theoretically the spectral profile of the transmitted optical power through the opaque silicon substrate [Ref. 23, Figs. 6 and 12]. Some degree of anticorrelation with the reflectance data is evident in those figures, especially for energies above 4 eV. However, a comparison of Powell's combined experimental – computational plots with Fig. 3 shows the distinct advantage of PAS as a sensitive technique for optical transmittance measurements on opaque samples.

The spectral dependence of the PAS signal magnitude from (100) silicon and SiO_2:Si has been thus far shown to be in agreement with the theoretical model developed in Part 2 (Figs. 2–4). Equation (38) for $r(\lambda)$ indicates that an essential result of the theory is that the seemingly unsaturated PAS signal from the SiO_2:Si system is generated from the wavelength dependence of $I_{\text{eff}}(\lambda)$. $r(\lambda)$ is the ratio of two real quantities, i.e., $I_{\text{eff}}^{(SiO_2:Si)}$ and $I_{\text{eff}}^{(Si)}$, each of which is phase-saturated, as shown in (37). Therefore, a necessary consequence of the theory is that $r(\lambda)$ should also be phase-saturated. Unlike conventional photoacoustic behavior [19], photoacoustic interferometry is expected to exhibit signal magnitude variations as a function of wavelength, *with no corresponding phase variations.* Figure 5 is a plot of the difference between PAS signal phases from an oxidized wafer ($L_1 = 5230$ Å, Fig. 4b) and the subsequently etched Si substrate: although individually there was a slight phase variation observed, it was traced to instrumental phase shifts. The difference $\Delta\phi = \phi_{SiO_2:Si} - \phi_{Si}$ is seen to be essentially independent of wavelength, in agreement with the predictions of our model.

4. Conclusions

A theoretical model for photoacoustic interferometry was developed and shown to be in agreement with experimental results from gate- and field-oxidized silicon. This work has demonstrated the feasibility of quantitative photoacoustic spectroscopy as a simple and sensitive thermal interferometric method for thin film transmittance measurements in the 9000 – 1000 Å range, with the potential to be extended to smaller thicknesses. Computer fits of the theory to PAS data are able to provide optimized thin film thickness estimates, which may be useful in microelectronic processing applications and other technological geometries for which reflectance measurements may be difficult or impossible to perform, such as thin films on non-reflecting substrates.

Acknowledgements. The authors wish to thank Mr. Dod Bhattiar of the Electrical Engineering Department, University of Toronto, for his valuable assistance with sample preparation.

References

1. P. Helander, I. Lundström: J. Appl. Phys. **52**, 1146 (1981)
2. L. Baldassarre, A. Cingolani: Solid State Commun. **44**, 705 (1982)
3. M. Morita: Jpn. J. Appl. Phys. **20**, 835 (1981)
4. Y. Fujii, A. Moritanti, J. Nakai: Jpn. J. Appl. Phys. **20**, 361 (1981)
5. M.J. Adams, B.C. Beadle, G.F. Kirkbright, K.R. Menon: Appl. Spectrosc. **32**, 430 (1978)
6. N.C. Fernelius: Appl. Surf. Sci. **4**, 401 (1980)
7. N.C. Fernelius: Appl. Opt. **21**, 481 (1982)
8. N.C. Fernelius: In *Laser Induced Damage in Optical Materials* (1979) Proceedings, 293 (1980)
9. A. Mandelis, Y.C. Teng, B.S.H. Royce: J. Appl. Phys. **50**, 7138 (1979)
10. N.C. Fernelius: In *Laser Induced Damage in Optical Materials* (1979) Proceedings, 301 (1980)
11. S.O. Kanstad, P.E. Nordal: Opt. Commun. **26**, 367 (1978)
12. M. Born, E. Wolf: *Principles of Optics*, 5th ed. (Pergamon Press, Oxford 1975) Chap. XIII
13. M. Born, E. Wolf: *Principles of Optics*, 5th ed. (Pergamon Press, Oxford 1975) Chap. VII
14. R.M.A. Azzam, N.M. Bashara: *Ellipsometry and Polarized Light* (North-Holland, Amsterdam 1977) Chap. 4
15. H.R. Phillip, E.A. Taft: Phys. Rev. **120**, 37 (1960)
16. S.M. Sze: *Physics of Semiconductor Devices* (Wiley, New York 1969) p. 54
17. F.A. McDonald: Am. J. Phys. **48**, 41 (1980)
18. C.A. Bennett, Jr., R.R. Patty: Appl. Opt. **21**, 49 (1982)
19. A. Rosencwaig, A. Gersho: J. Appl. Phys. **47**, 64 (1976)
20. Y.S. Touloukian, R.W. Powell, C.Y. Ho, M.C. Nicolasu: *Thermal Diffusivity* (IFI/Plenum Press, New York 1973)
21. R.B. Laughlin: Phys. Rev. B **22**, 3021 (1980)
22. I.H. Malitson: J. Opt. Soc. Am. **55**, 1205 (1965)
23. R.J. Powell: J. Appl. Phys. **40**, 5093 (1969)